

# SINTEZA ȘI CARACTERIZAREA PULBERILOR HIBRIDE NANOCOMPOZITE OBȚINUTE PRIN ALIERE MECANICĂ

## SYNTHESIS AND CHARACTERIZATION OF HYBRID NANOCOMPOSITE POWDERS VIA MECHANICAL ALLOYING

A. CANAKCI\*, T. VAROL, H. CUVALCI, F. ERDEMIR, S. OZKAYA

<sup>a</sup>Department of Metallurgical and Materials Engineering, Engineering Faculty, Karadeniz Technical University

*In this study, novel CuSn10-B<sub>4</sub>C-graphite hybrid nanocomposite powders were synthesized by the solid-state powder processing technique of mechanical alloying. The effects of the addition of graphite particles, B<sub>4</sub>C distribution and milling time on the morphology, particle size and microstructure of CuSn10-graphite nanocomposite powders were investigated. It was found that the particle size of the nanocomposite powders was significantly lower than those of the CuSn10 alloy powders. Electron microscopy studies confirmed the formation of equiaxed graphite with a wide size distribution in the range of 100 to 200 nm.*

**Keywords:** Mechanical alloying, Nanocomposite powders, Morphology, Electron microscopy

### 1. Introduction

Cu-based alloys or composites are used for high electric and thermal conductive application, namely, vacuum contact interrupter, high-performance switches, spot welding electrodes, rotating source neutron targets, combustion chamber liners, nozzle liners, aerospace propulsion systems and fusion power plants [1]. Moreover, copper is widely used for many applications such as electrical contacts (Cu-Cr, Cu-Ag), electronic packaging and resistance welding electrodes. However, low mechanical strength and undesirable wear resistance limit the application fields of copper [2, 3].

CuSn bronzes have been used for a long time in many tribological fields on account of their self-lubricating, high strength and corrosion resistance properties as well as high wear resistance and hardness. In these alloys, Sn was used at a 4-10 wt.%. These types of bronzes have been used in chemical industry, navigation, pivots, springs in machine production, gears against corrosion resistance, and crank pivot bearings [4]. Cu-based composites are extensively used in friction devices of various machines and mechanisms because of good heat conductivity, wear resistance, and stable chemical properties. Solid lubricants can be added into Cu matrix to improve its wear resistance. Solid lubricant-rich films could be produced between contact surfaces in friction process because of the lamellar structure and softness of these solid lubricants. Graphite as solid lubricants is widely used due to its low cost and excellent lubrication performance [5]. Copper-graphite composite may

be a tribological composite produced through powder metallurgy (P/M) route and can be used in sliding electrical contact applications requiring low friction and wear in addition to high electrical conductivity [6]. The desired material properties from the electrical contact and motor brush are excellent electrical conductivity, resistance electric arc corrosion, high mechanical strength and wear resistance. However, all of these desired features can be achieved with the hybrid composites.

Mechanical alloying (MA) has been used to synthesize metal matrix composites due to the relative ease of the process and low processing cost [7]. The mechanical alloying process consists of repeated welding-fracturing-welding of a mixture of initial powders in a high-energy ball mill [8-10].

The need for a new wear resistant material for high performance tribological applications has been one of the major driving forces for the tribological development of hybrid composites. The aim of this research is to investigate the possibility of fabricating novel CuSn10-B<sub>4</sub>C-graphite nanocomposites with improved B<sub>4</sub>C and graphite distribution. The graphite content is varied from 1 to 5 wt.% to study the role of graphite in refining the morphology, microstructure, particle size and in promoting the nanocomposite formation.

### 2. Experimental

High purity CuSn10 powder (Alfa-Aesar, Germany) with mean particles size of 28 μm, B<sub>4</sub>C powders (Alfa-Aesar, Germany) with particles size of 49 μm and graphite powders (Alfa-Aesar, Germany) with particles size of 30 μm were used

\* Autor corespondent/Corresponding author,  
E-mail: aykut@ktu.edu.tr

as the starting materials. Mechanical alloying was carried out in a planetary ball mill (Fritsch "Pulverisette 7, Premium line") using tungsten carbide container and balls. A total of 25 g powder with no process control agent was used in all MA runs. The hybrid nanocomposite powders were produced with different graphite particles weight percentages (0, 1, 3 and 5 wt.%), milling times (0.5, 1, 2, 5, 8, 12 and 24h) and ball-to-powder weight ratios (10:1). Ball diameter (10 mm) and speed (400 rpm) were kept constant in all the experiments. The composition of the synthesized composites is given in Table 1.

**Table 1**  
The compositions of fabricated composites.

Sample	Composition (wt.%)		
	CuSn10	B <sub>4</sub> C	Graphite
1	90	10	0
2	89	10	1
3	87	10	3
4	85	10	5

The particle size of the as-received and milled powders were quantified using a laser particle size analyzer (Malvern, model 'Mastersizer Hydro 2000e'). Morphology and microstructure investigations of the composite powders were carried out using a scanning electron microscope (SEM) (Zeiss Evo LS10). EDX line scan analysis was employed to quantitatively determine the B<sub>4</sub>C distribution. The phase analysis of milled products was evaluated by X-ray diffraction (XRD) (Rigaku Corporation, Japan) using CuK $\alpha$  radiation (1.5406 Å) operating at 30 mA and 40 kV. The XRD patterns were recorded in the range of 20°–100° with a set scanning speed of 2°/min.

### 3. Results and discussion

#### 3.1. Morphological evaluations

The initial morphologies of CuSn10 alloy, graphite and B<sub>4</sub>C particles are shown in Figure 1. The change in the morphology of powder particles was studied by SEM. SEM images of the milled powders at different times are shown in Figures 2a-e. In the early stage of milling (0.5 h), the CuSn10 particles, which are irregular in shape, undergo a significant plastic deformation. As it is seen in Figure 2a, after 0.5 h milling, the morphology and size of milled powders have markedly changed when compared to the starting powders. The morphology of the milled powders had changed into flake shape (Fig. 2a). It should be noted that the flake morphology caused by ball-powder-ball collision increases particle size of the milled powders. Moreover, the B<sub>4</sub>C and graphite particles tended to embed into the CuSn10 matrix

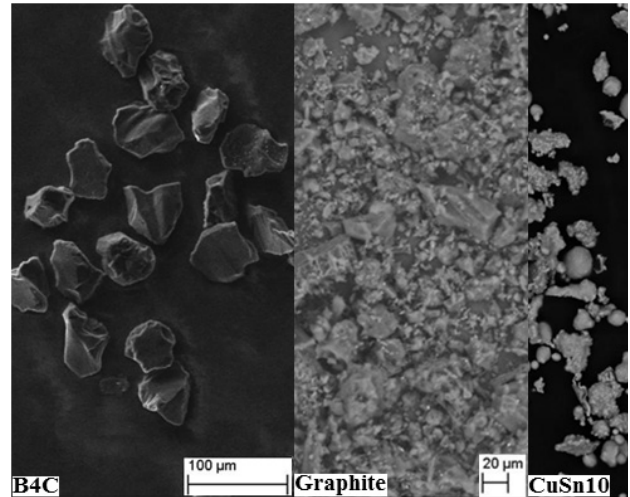
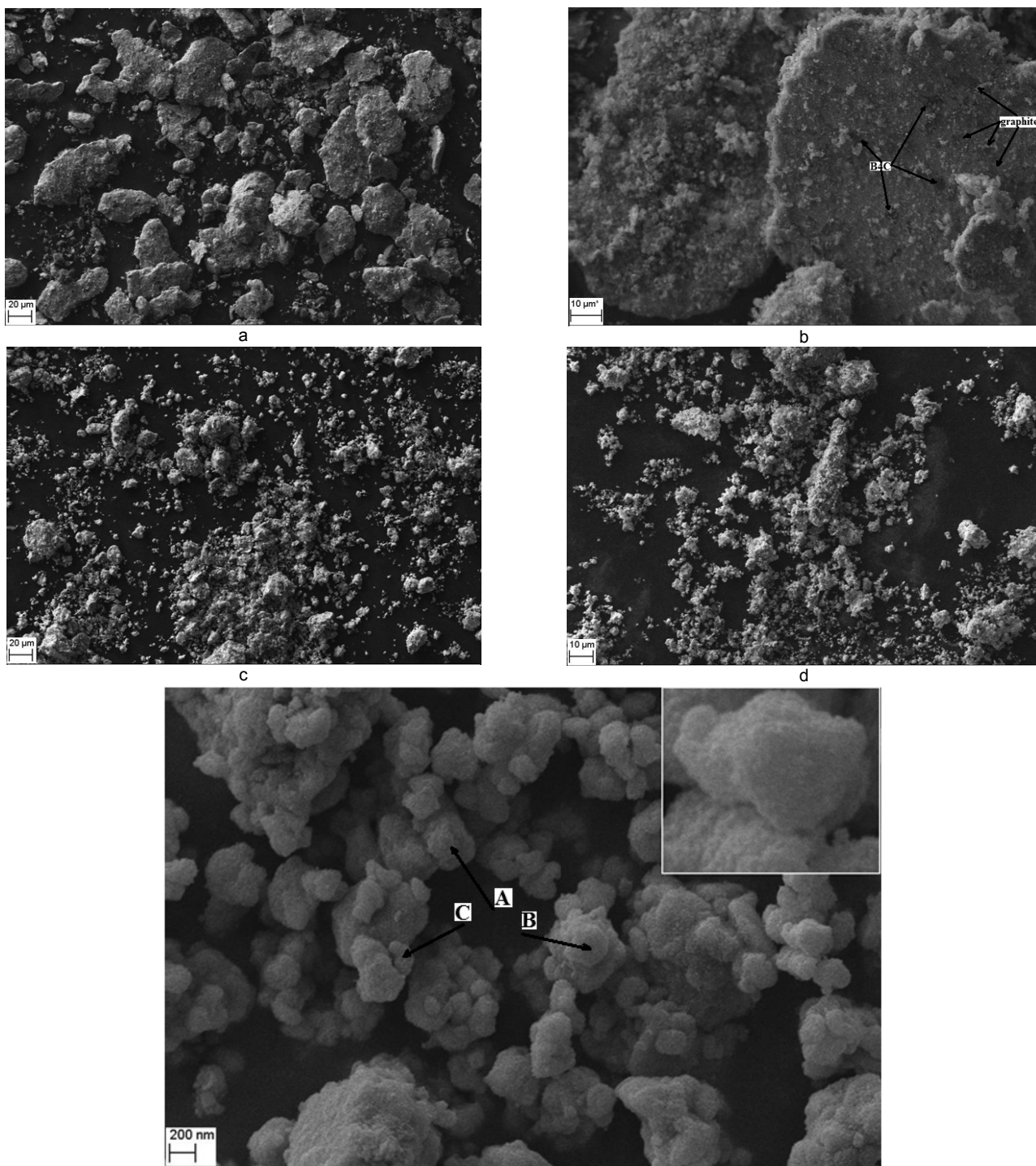


Fig. 1 - SEM micrograph which showing the particle shape of initial powders.

powders (Fig. 2b) at this early stage of milling (up to 2h). It was observed that the mixing of CuSn10 and B<sub>4</sub>C-graphite is not well distributed due to the relative short milling time. In other words short milling times was not enough for homogenous distribution of reinforcement particles [11, 12]. Continuous and severe repetitive impacts of the milling media in longer milling times (5 h) caused flaky particles to break into smaller particles (Fig. 2c) [12]. However, flaky particles can still be seen in the milled powders. After 5 h milling, these flaky particles were work-hardened resulting in the activation of fracture mechanism (Fig. 2d). Eventually, when the milling time increased to 24 h (Fig. 2e) a balance was established between the cold welding and fracturing events and a steady-state situation was obtained. It means that the distribution of B<sub>4</sub>C and graphite particles in the CuSn10 matrix was very uniform at this stage. Also, the average particles size of CuSn10-10wt.% B<sub>4</sub>C-5wt.% Graphite powder after 24 h milling is 50-200 nm (Fig. 2e). In all cases, a similar trend in powder particle size was observed - i.e. an initial increase is followed by a decrease and then steady state. This behavior can be attributed to the cold welding of initial ductile particles followed by work hardening and thus the fracturing of powder particles. When the rate of cold welding and fracturing processes equals, the steady state is achieved [13]. Although process control agent was not used in the mechanical alloying process, graphite prevented excessive cold welding between ductile particles and ball-vial surfaces. Therefore, it can be inferred that graphite acted as a process control agent. It was also observed that powder agglomeration decreased with the increase in milling time because of the reduction in particle size (Fig. 2e). The agglomeration and growth of the nanoparticles can be attributed to the surface free energy of the nanoparticles [14].



Element wt. %

	Copper	Tin	Boron	Carbon
A	67.53	7.54	10.29	14.64
B	80.04	11.7	3.32	4.94
C	78.08	10.02	8.3	3.6

e

Fig. 2 - SEM images of the CuSn<sub>10</sub>-B<sub>4</sub>C-graphite (5wt.%) nanocomposite powders after (a, b) 0.5h, (c) 5 h, (d) 12 h and (e) 24h of milling.

### 3.2. Particle size

In the first stage of mechanical alloying process, brittle reinforcement particles begin to break while ductile matrix powder transforms flake

morphology due to plastic deformation (ball-powder-ball and ball-powder-vial surface collisions) [15]. Then fractured brittle particles embedded into ductile and flake shape matrix

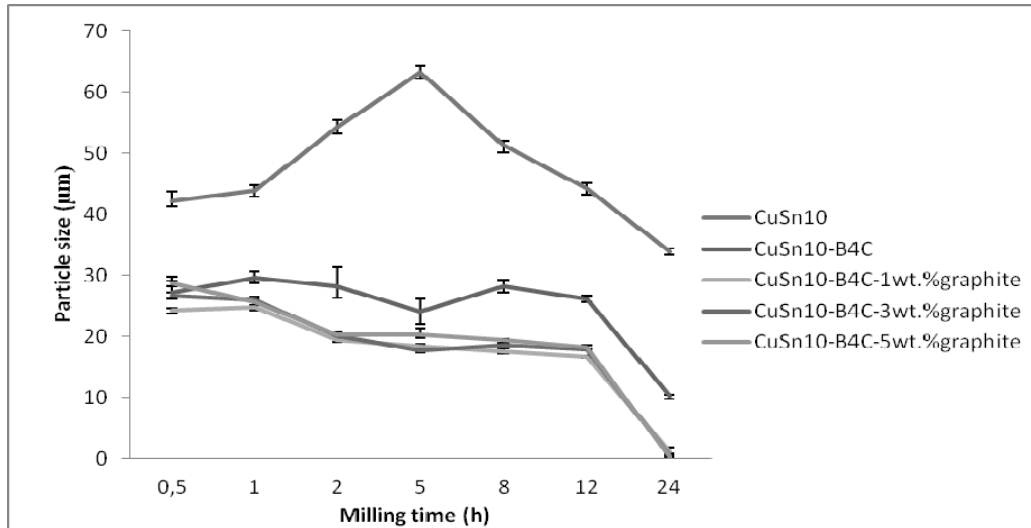


Fig. 3 - Particle size of nanocomposite powders as a function of the milling time.

powders due to cold welding [16]. The deformation of matrix and reinforcement particles due to ball-powder-ball and ball-powder-vial surface collisions increased the fracture process and then particle morphology of nanocomposite particles transformed equiaxed morphology [15].

The average particle size of milled CuSn10-B<sub>4</sub>C-Graphite powders versus milling time is shown in Figure 3. The particle size changed with milling time due to cold welding and fracturing of powder articles. While cold welding increased the particle size, fracturing reduced the size. In the early stages of milling, the powder particles are still soft and cold welding predominates [17, 18]. It seems that the cold welding was the dominant mechanism during the milling period of 0.5- 2 h due to the ductility of CuSn10 powders. Consequently, the particle size increased (Fig. 3). Mixing with the B<sub>4</sub>C and graphite particles also could increase the brittleness of CuSn10 matrix powders and consequently the rate of fracturing. Hence, with the increase in the milling time the particles get work hardened became more brittle and their fracture led to a reduction in particle size. Thus, the rate of fracturing tended to increase with the increase in the milling time which can be clearly seen in Figure 3. When the graphite content was low, the CuSn10 particle deformation and cold welding were the predominant mechanisms. By increasing the graphite content, contribution of the fracture mechanism was increased and consequently the particle size was more decreased (Fig. 3). As can be seen in Figure 3, particle size was stable after steady state conditions in mechanical alloying process. In this stage, a balance was established between the cold welding and the fracturing process for a milling time of 24h. Finally, in the fourth stage, the average particle size almost remained constant.

### 3.3. Effect of milling time on the distribution of reinforcement particles

During the first stage of mechanical alloying, the morphology of CuSn10 particles changed from irregular to flatten due to the plastic deformation by ball-powder-ball and ball-powder-vial surface. The distribution of B<sub>4</sub>C particles was not homogeneous due to irregular embedded into CuSn10 powders and not embedded B<sub>4</sub>C particles in this stage. In the following stages, the flattened particles welded to each other, hardened and fractured. Simultaneously, the reinforcing particles (B<sub>4</sub>C and graphite) also were broken and became embedded in the CuSn10 powders. After 24 h of milling, the process was completed and the distribution was homogeneous. This indicated that distribution of reinforcing particles during mechanical alloying process was not only dependent on ball to powder ratio, milling speed and process control agent but also milling time and on the milling system (ductile-ductile or ductile-brittle). EDX analysis was performed to follow the distribution of B<sub>4</sub>C particles on the composite powders. Figure 4 shows the EDX analysis along the arrow lines from the left of the right. EDX line scan analysis results revealed that mechanical alloying technique provided homogenous distribution of B<sub>4</sub>C particles within CuSn10 alloy powders.

### 3.4. X-Ray diffraction analysis

Figure 5 shows XRD patterns of the powders milled for various times, revealing the structural evolution of the powder mixture as milling progressed. By increasing the milling time, the peaks were gradually broadened and their intensities decreased. These observations were found in agreement with the studies reported for other metal matrix composites [19]. Analysis of the XRD

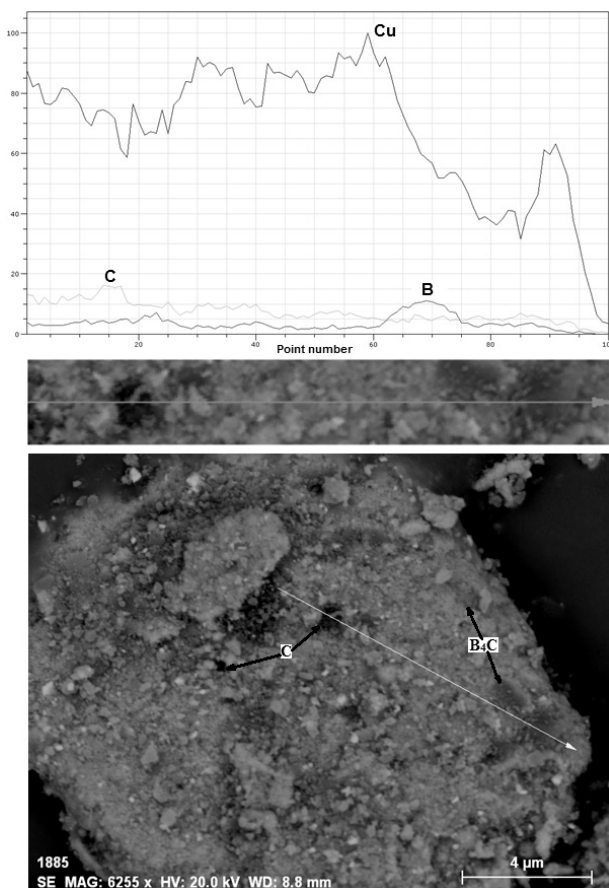


Fig. 4. - EDX line scans result showing distributions of  $B_4C$  particles.

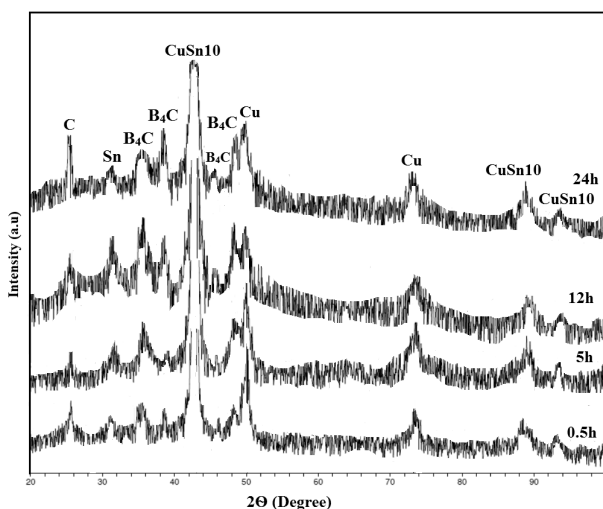


Fig. 5. - XRD patterns of  $CuSn_{10}$ - $B_4C$ -graphite (5wt.%) nanocomposite powders after 0.5 h, 5 h, 12 h and 24 h of milling.

patterns revealed that up to 24 h milling, gradual grain refinement was the only considerable change occurring in the powder mixture and no detectable reaction took place.

## 4. Conclusions

In this study, novel  $CuSn_{10}$ - $B_4C$ -Graphite nanocomposite powders were synthesized by mechanical alloying process. The conclusions can be summarized as following:

1. If optimized process parameters have been selected, mechanical alloying technique is suitable technique for nanoparticles and nanocomposite powders.

2. With the increase in the milling time, graphite content and  $B_4C$  particles, the particle size of  $CuSn_{10}$ - $B_4C$ -Graphite nanocomposite powders decreased. The average particles size of  $CuSn_{10}$ - $B_4C$ -5wt.% Graphite powder after 24 h milling was about 100-200 nm.

3. It was found that the addition of graphite and  $B_4C$  particles had a graphite influence on the powder morphology. Particle agglomeration was observed in nanocomposite powders probably due to the surface free energy of the nanoparticles.

4-Graphite acted as a process control agent and prevented excessive cold welding in the mechanical alloying process.

## Acknowledgments

The authors are grateful to the Karadeniz Technical University Research Foundation for financially supporting this research (No: 2010.112.0105).

## REFERENCES

1. S. Mula, P. Sahani, S.K. Pratihari, S. Mal and C.C. Koch, Mechanical properties and electrical conductivity of  $Cu-Cr$  and  $Cu-Cr-4\%$   $SiC$  nanocomposites for thermo-electric applications. *Materials Science and Engineering A*, 2011, **528**, 4348.
2. M. Barmouza, M. Kazem, B. Givi and J. Seyfi, On the role of processing parameters in producing  $Cu/SiC$  metal matrix composites via friction stir processing: Investigating microstructure, microhardness, wear and tensile behavior. *Materials Characterization*, 2011, **62**, 108.
3. D.Y. Ying, D.L. Zhang, Processing of  $Cu-Al_2O_3$  metal matrix nanocomposite materials by using high energy ball milling *Materials Science and Engineering A*, 2000, **286**, 152.
4. O. Yilmaz and H. Turhan, The relationships between wear behavior and thermal conductivity of  $CuSn/M7C3-M23C6$  composites at ambient and elevated temperature. *Composite Science and Technology*, 2001, **61**, 2349.
5. B. Chen, Q. Bi, J. Yang, Y. Xia and J. Hao, Tribological properties of solid lubricants (graphite, h-BN) for  $Cu$ -based P/M friction composites. *Tribology International*, 2008, **41**, 1145.
6. R. G.Chandrananth, K. Rajkumar, S. Aravindan, Fabrication of copper-TiC-graphite hybrid metal matrix composites through microwave processing. *International Journal of Advanced Manufacturing Technology*, 2010, **48**, 645.
7. V. Viswanathan, T. Laha, K. Balani, A. Agarwal, S. Seal, Challenges and advances in nanocomposite processing techniques, *Materials Science and Engineering R*, 2006, **54**, 121.
8. J.B. Fogagnolo, F. Velasco, M.H. Robert, J.M. Torralba, Effect of mechanical alloying on the morphology, microstructure and properties of aluminium matrix composite powders. *Materials Science and Engineering A*, 2003, **342**, 131.

9. X.T. Luo, G.J. Yang, C.J. Li, Preparation of cBNp/NiCrAl nanostructured composite powders by a step-fashion mechanical alloying process. Powder Technology 2012, **217**, 591.
10. G.K. Williamson, W.H. Hall, X-ray line broadening from filed aluminium and wolfram. Acta Metallurgica, 1953, **1**, 22.
11. J. Li, F. Li and K. Hu, Preparation of Ni/Al<sub>2</sub>O<sub>3</sub> nanocomposite powder by high-energy ball milling and subsequent heat treatment. Journal of Materials Processing Technology, 2004, **147**, 236.
12. M. Hedayati, M. Salehi, R. Bagheri, M. Panjepour and A. Maghziyan, Ball milling preparation and characterization of poly (ether ether ketone)/surface modified silica nanocomposite, Powder Technology, 2011, **207**, 296.
13. S.A. Khadem, S. Nategh and H. Yoozbashizadeh, Structural and morphological evaluation of Al-5 vol.%SiC nanocomposite powder produced by mechanical milling, Journal of Alloys and Compounds, 2011, **509**, 2221.
14. A.J. Song, M.Z. Ma, W.G. Zhang, H.T. Zong, S.X. Liang, Q.H. Hao, R.Z. Zhou, Q. Jing and R.P. Liu, Preparation and growth of Ni-Cu alloy nanoparticles prepared by arc plasma evaporation. Materials Letters 2010, **64**,1229.
15. M.F. Zawrah, H. Abdel-kader and N.E. Elbaly, Fabrication of Al<sub>2</sub>O<sub>3</sub>-20 vol.% Al nanocomposite powders using high energy milling and their sinterability. Materials Research Bulletin, 2012, **47**, 655.
16. A. Canakci, T. Varol, S. Ertok, The effect of mechanical alloying on Al<sub>2</sub>O<sub>3</sub> distribution and properties of Al<sub>2</sub>O<sub>3</sub> particle reinforced Al-MMCs. Science and Engineering of Composite Materials, 2012, **19**, 227.
17. B. Prabhu, C. Suryanarayana, L. An and R. Vaidyanathan, Synthesis and characterization of high volume fraction Al-Al<sub>2</sub>O<sub>3</sub> nanocomposite powders by high-energy milling. Materials Science and Engineering A, 2006, **425**, 192.
18. A. Canakci, S. Ozsahin and T. Varol, Modeling the influence of a process control agent on the properties of metal matrix composite powders using artificial neural networks. Powder Technology, 2012 **228**, 26.
19. H. Abdoli, E. Salahi, H. Farnoush and K. Pourazrang, Evolutions during synthesis of Al-AlN-nanostructured composite powder by mechanical alloying. Journal of Alloys and Compounds, 2008, **461**,166.

\*\*\*\*\*

## MANIFESTĂRI ȘTIINȚIFICE / SCIENTIFIC EVENTS

**14<sup>th</sup>** INTERNATIONAL CONFERENCE  
**European Ceramic Society**

21-25 JUNE, 2015 | Toledo, España



Organised every two years, the ECeRS Conference is the place to be for scientists, students and industrialists willing to have a direct access to one of the largest community of international experts of ceramic science and technology.

The conference will be organised around seven general themes that cover most aspects of ceramic science and technology, "Innovative processing and synthesis", "High temperature processes and advanced sintering", "Ceramics and glasses for healthcare", "Ceramics for energy production and storage", "Advanced structural ceramics", "Ceramics for electro-magnetic and optical applications" and "Traditional ceramics, Innovative construction materials and Cultural heritage". Focused symposia dealing with specific issues, such as "Refractories", will also be organized.

Contact: <http://www.ecers2015.org/>

\*\*\*\*\*